Pergamon

Int. J. Solids Structures Vol. 35, Nos 34–35, pp. 4739–4751, 1998

Printed in Great Britain
0020–7683/98/$—see front matter

PII: S0020–7683(98)00092–4

DYNAMIC POROELASTICITY OF THINLY LAYERED STRUCTURES

S. GELINSKY†
Western Atlas Logging Services, 10201 Westheimer, Houston, Texas 77042, U.S.A.

S. A. SHAPIRO
Nancy School of Geology (ENSG/INPL) & CRPG, Batiment G, Computer Science Department, Rue du Doyen-Marcel-Roubault, BP40 54501 Vandoeuvre les Nancy, France and Wave Inversion Technology Group, Geophysical Institute, Karlsruhe University, Hertzstr. 16, D-76187 Karlsruhe, Germany

T. MÜLLER
Wave Inversion Technology Group, Geophysical Institute, Karlsruhe University, Hertzstr. 16, D-76187 Karlsruhe, Germany

and

B. GUREVICH
Geophysical Institute of Israel, P.O. Box 2286, Holon 58122, Israel

(*Received* 5 *May* 1997; *in revised form* 2 *September* 1997)

Abstract—Compressional seismic *P*-waves, propagating in poroelastic, fluid saturated, laminated sediments are strongly affected by the medium heterogeneity. Here, simple analytical expressions for the *P*-wave phase velocity and attenuation coefficient are derived. Both are functions of frequency and statistical medium parameters such as correlation lengths and variances. The theoretical results are compared with results from numerical simulations and show good agreement. In heterogeneous media, impedance fluctuations lead to poroelastic scattering; variations of the layer compressibilities cause inter-layer flow (a 1-D macroscopic local flow). From the seismic frequency range (10–100 Hz) up to ultrasonic frequencies, attenuation due to heterogeneity is strongly enhanced compared to homogeneous Biot models. The new theory automatically includes different asymptotic approximations, such as poroelastic Backus averaging in the quasi-static and the no-flow limit, geometrical optics, and intermediate frequency ranges.

INTRODUCTION

A seismic wave in randomly heterogeneous elastic media faces multiple scattering and is exponentially attenuated due to coherent backscattering even without the presence of any dissipative mechanism (Sheng, 1995). Additionally, in porous saturated rocks a propagating wave causes fluid flow that leads to an extra attenuation. In homogeneous media this dissipation is caused by the relative movement between the solid matrix and the fluid, the so-called Biot global flow (Biot, 1962). The Biot theory predicts the existence of two compressional waves in porous saturated rock, a normal P_1-mode and the highly attenuated P_2-mode, the so-called slow wave.

In heterogeneous media, seismic waves that propagate through a stack of layers with variable compliances may additionally cause inter-layer flow of pore fluid across interfaces from more compliant into stiffer layers (White, 1983; Norris, 1993; Gurevich and Lopatnikov, 1995). Below a characteristical frequency ω_0 defined in eqn (5), in the quasi-static limit, the fluid pressure is equilibrated between adjacent layers due to viscous fluid motion across the layer boundaries (excitation of diffusive Biot-slow waves at the interfaces,

† Author to whom correspondence should be addressed. Tel.: 001 713 972 6511. Fax: 001 713 972 6658. E-mail: Stephan.gelinsky@waii.com

Chandler and Johnson, 1981). The generation of propagating Biot slow waves at a permeable interface has been observed in several laboratory experiments at ultrasonic frequencies above ω_0 (Plona, 1980; Rasolofosaon, 1988). In this no-flow limit the layers behave like isolated since for these frequencies the fluid pressure is no longer equilibrated by fluid diffusion across interfaces.

Even if the layers are virtually isolated, open-pore boundary conditions are the only ones which are in accordance with a consistent use of Biot theory for the whole medium, including surfaces for which the medium parameters are discontinuous (Gurevich and Schoenberg, 1997, 1998). According to the same study, poroelastic media with closed or partially open interfaces can be modeled by replacing such an interface with a thin poroelastic layer with permeability proportional to its thickness d and taking the limit $d \to 0$. The proportionality constant is defined as a measure of the hydraulic permeability of the original interface, ranging from zero for closed interfaces to infinity for open ones.

While each of these attenuation mechanisms has been studied before, here a comprehensive theory is presented that comprises all three mechanisms and their interactions. The new theory (first proposed by Gelinsky and Shapiro, 1997a) is a poroelastic extension of the generalized O'Doherty–Anstey formalism for elastic waves in multilayered media (Shapiro and Hubral, 1996). Predictions by the new theory are compared with numerical results that were derived using a propagator matrix method (also called layer code or the Thompson–Haskell method; Schmidt and Tango, 1986). Both theoretical and numerical calculations are consistently performed using open-pore boundary conditions.

STATISTICAL MODEL

The poroelastic generalized O'Doherty–Anstey theory is a small perturbation approach that describes statistically the heterogeneous medium. The medium parameters (represented as $X = X_0(1+\varepsilon_X(z))$, consisting of background X_0 and fluctuations $\varepsilon_X(z)$), are the poroelastic constants, rock density ϱ, porosity φ, permeability k, and the fluid properties: viscosity η, density ϱ_f, and the bulk modulus K_f. It is assumed that the first moment of the fluctuations $\langle\varepsilon\rangle = 0$ and moments $\langle\varepsilon^n\rangle$ higher than the second one are small and thus can be neglected. Yet the theory may work remarkably well even for rather strong fluctuations of more than 20% (the exact limiting values are the same as in the elastic case and given in Shapiro and Hubral, 1996). Fluctuations of permeability can be much larger than 20%. These fluctuations affect the global flow attenuation and are important only for frequencies of the order of Biot's critical frequency ω_c defined in eqn (4) (for more details on permeability fluctuations, see Shapiro and Müller, 1998). Practical applications of the new theory comprise the analysis of surface seismic-, VSP-, and borehole acoustic data. These measurements generally are performed in a frequency range well below ω_c so that this is not a strong limitation.

Throughout this paper, the brackets denote averaging over the statistical ensemble, i.e., over many realizations of the random medium under consideration. In practice, there exists only one set of logs providing the parameters of the one medium that is studied, and spatial averaging can be used to find the auto- and cross-correlation functions of the fluctuations. The results that we obtain characterize the wave propagation in a single typical realization of the medium. The correlation function can be written as the product of a function $\Phi(\delta/a)$ which depends on the depth increment δ and correlation length a and of the variances $\sigma^2_{XY}(\delta = 0) = \sigma^2_{XY}$. The correlation functions are defined by:

$$\sigma^2_{XX}(\delta) = \langle\varepsilon_X(z)\varepsilon_X(z+\delta)\rangle = \frac{1}{L}\int_0^L \varepsilon_X(z)\varepsilon_X(z+\delta)\,\mathrm{d}z,$$

$$\sigma^2_{XY}(\delta) = 1/2(\langle\varepsilon_X(z)\varepsilon_Y(z+\delta)\rangle + \langle\varepsilon_X(z+\delta)\varepsilon_Y(z)\rangle). \tag{1}$$

Here, a is the correlation length of the fluctuations. A typical stack of random layers is supposed to be thick enough to cause self-averaging of the P-wave's vertical phase increment

and of its attenuation coefficient—the averaging is performed in the process of wave-propagation (references in Shapiro and Hubral, 1996).

THEORY

The starting point to describe layered poroelastic media is the system of Biot's equations (Biot, 1962). For vertically propagating plane waves, these equations are transformed into first-order differential matrix equations. This is done in analogy to the elastic case described by Aki and Richards (1981). The transformed Biot equations read:

$$\frac{d\vec{\zeta}}{dz} + \mathbf{P}\vec{\zeta} = 0. \tag{2}$$

The wavefield parameters are contained in the vector $\vec{\zeta} = (u_z, \tau_{zz}, w_z, p_f)^T$. Its elements are the vertical displacement of the solid phase, u_z, the corresponding relative displacement of the solid and the fluid phase, multiplied by porosity, w_z, the vertical stress τ_{zz}, and the fluid pressure p_f. All are functions of depth. The matrix $\mathbf{P}$, containing all information about the medium, is given by:

$$\mathbf{P} = \begin{bmatrix} 0 & \frac{1}{P_d} & 0 & \frac{\alpha}{P_d} \\ -\varrho\omega^2 & 0 & -\varrho_f\omega^2 & 0 \\ 0 & -\frac{\alpha}{P_d} & 0 & -\frac{1}{M} - \frac{\alpha^2}{P_d} \\ \varrho_f\omega^2 & 0 & i\omega\tilde{q} & 0 \end{bmatrix}, \tag{3}$$

where $P_d = K_d + \frac{4}{3}\mu_d$ is the dry P-wave modulus, K_d and μ_d are the bulk and shear moduli (throughout this paper, the subscripts d, g, f denote properties of the dry frame, of the grain material, and of the fluid, respectively); $H = P_d + \alpha^2 M$ is the saturated P-wave modulus, with α and M defined by: $\alpha = 1 - (K_d/K_g)$ and $M = [(\varphi/K_f) + [(\alpha - \varphi)/K_g)]^{-1}$. The constant N is defined as $N = MP_d/H$. The permeability k and viscosity η enter the theory via the Darcy coefficient $\tilde{q} = \eta/k$ which appears with an extra frequency factor in eqn (3). With these parameters, Biot's critical frequency is given by:

$$\omega_c = \frac{\eta\varphi}{k\varrho_f}, \tag{4}$$

and the characteristic frequency separating the inter-layer flow and the no flow regime is defined by

$$\omega_0 = \frac{kN}{\eta a^2}. \tag{5}$$

It is strongly dependent on the correlation length a of the medium heterogeneity.

The matrix $\mathbf{P} = \mathbf{P}_0 + \mathbf{P}_\varepsilon$ consists of a homogeneous background part $\mathbf{P}_0$ and a part $\mathbf{P}_\varepsilon$ that describes fluctuations. The eigenvalues of $\mathbf{P}_0$ are $i\tilde{\kappa}_1$ and $i\tilde{\kappa}_2$ ($\tilde{\kappa}_1$, $\tilde{\kappa}_2$ are the complex wavenumbers of Biot's fast and slow compressional wave, respectively). Taylor expansion in the small fluctuations ε_χ, keeping only terms up to second order in ε, yields the fluctuation matrix $\mathbf{P}_\varepsilon$. Diagonalization of the matrix $\mathbf{P}_0$ is done by a linear transformation $\mathbf{P}_0' = \mathbf{E}_0^{-1} \cdot \mathbf{P}_0 \cdot \mathbf{E}_0$. Here, $\mathbf{E}_0$ is the eigenvector matrix of $\mathbf{P}_0$, and $\mathbf{E}_0^{-1}$ its inverse. The resulting matrix reads:

$$\mathbf{P}_0' = \begin{bmatrix} i\tilde{\kappa}_1 & 0 & 0 & 0 \\ 0 & i\tilde{\kappa}_2 & 0 & 0 \\ 0 & 0 & -i\tilde{\kappa}_1 & 0 \\ 0 & 0 & 0 & -i\tilde{\kappa}_2 \end{bmatrix}. \tag{6}$$

Next, $\mathbf{P}_\varepsilon$ is replaced by $\mathbf{P}_\varepsilon' = \mathbf{E}_0^{-1} \cdot \mathbf{P}_\varepsilon \cdot \mathbf{E}_0$. The elements of $\mathbf{P}_\varepsilon'$ can be expressed by eight known combinations of the medium fluctuations, $c_1, \ldots, c_8$ and reads:

$$\mathbf{P}' = \mathbf{P}_0' + \mathbf{P}_\varepsilon' = \begin{bmatrix} i\tilde{\kappa}_1 + c_1 & c_2 & c_3 & c_4 \\ c_5 & i\tilde{\kappa}_2 + c_6 & c_7 & c_8 \\ -c_3 & -c_4 & -i\tilde{\kappa}_1 - c_1 & -c_2 \\ -c_7 & -c_8 & -c_5 & -i\tilde{\kappa}_2 - c_6 \end{bmatrix}. \tag{7}$$

Finally, the wavefield vector is transformed, $\vec{\xi} = \mathbf{E}_0^{-1}\zeta$. The elements of $\vec{\xi} = (d_1, d_2, u_1, u_2)^T$, which is continuous across interfaces, are for the homogeneous background medium the displacements caused by down- and up-going waves of type 1 and 2, respectively. Thus, eqn (2) is transformed to:

$$\frac{\mathrm{d}\vec{\xi}}{\mathrm{d}z} + (\mathbf{P}_0' + \mathbf{P}_\varepsilon')\vec{\xi} = 0. \tag{8}$$

In the following, it is assumed that the fluctuations and, therefore, the elements of P_ε' are small and that system (8) can be solved by a small perturbation expansion. This yields the time-harmonic transmissivity T for a stack of layers with the thickness L as a function of the eigenvalues of $\mathbf{P}_0$ and of the elements of $\mathbf{P}_\varepsilon'$. For vertical incidence,

$$T = \exp\left[i(\Psi L - \omega t) - \gamma L\right] \tag{9}$$

describes the transmission of a compressional plane wave through a stack of thin layers with the total thickness L between two homogeneous halfspaces on its top and bottom. The P_1-wave phase velocity, $V_P = \omega/\Psi$, and the attenuation coefficient γ can be calculated from T.

The next steps to derive the transmissivity are performed in analogy to the purely elastic case (Shapiro and Hubral, 1996). However, now there is an interaction between the fast P_1-wave and the strongly attenuated P_2-wave (due to the heterogeneity of the layered medium). This interaction is similar to that between P- and SV-waves for purely elastic heterogeneous media in the case of oblique incidence. The following boundary conditions are considered: $d_1(z=0) = 1$, $d_2(z=0) = 0$, $u_1(z=L) = 0$, $u_2(z=L) = 0$. At $z = 0$ only a down-going fast P_1-wave is given. In the depth interval $0 < z < L$, however, d_2, u_1, and u_2 are not equal to zero because of the internal scattering processes caused by the heterogeneity. Integrating eqn (8), using the boundary conditions, and keeping only fluctuations of first-order, the first approximations (superscript 1st) for the down- and up-going waves are obtained:

$$d_1^{1\mathrm{st}}(z) = \exp\left(i\tilde{\kappa}_1 z + \int_0^z c_1^{1\mathrm{st}}(z')\,\mathrm{d}z'\right),$$

$$d_2^{1\mathrm{st}}(z) = \exp(i\tilde{\kappa}_2 z)\int_0^z c_5^{1\mathrm{st}}(z')\exp(-i\tilde{\kappa}_- z')\,\mathrm{d}z',$$

$$u_1^{1\mathrm{st}}(z) = \exp(-i\tilde{\kappa}_1 z)\int_z^L c_3^{1\mathrm{st}}(z')\exp(2i\tilde{\kappa}_1 z')\,\mathrm{d}z',$$

$$u_2^{\mathrm{1st}}(z) = \exp(-i\tilde{\kappa}_2 z)\int_z^L c_{c_7}^{\mathrm{1st}}(z')\exp(i\tilde{\kappa}_+ z')\,\mathrm{d}z'. \tag{10}$$

Here, we defined $\tilde{\kappa}_+ = \tilde{\kappa}_2+\tilde{\kappa}_1$, and $\tilde{\kappa}_- = \tilde{\kappa}_2-\tilde{\kappa}_1$. To calculate the transmissivity of the P_1-wave only the second-order approximation of d_1 is needed. Further, to obtain the phase velocity and the attenuation coefficient of the dynamic equivalent medium, the logarithm of the transmissivity must be analyzed. For this it is convenient to rewrite the first equation of system (8):

$$\frac{\partial(r^{\mathrm{R}}+ir^{\mathrm{I}})}{\partial z} = i\tilde{\kappa}_1 + c_1(z) + c_3(z)\frac{u_1(z)}{d_1(z)} + c_2(z)\frac{d_2(z)}{d_1(z)} + c_4\frac{u_2(z)}{d_1(z)}, \tag{11}$$

where r^{R} and r^{I} denote the real and imaginary parts of $\ln(d_1)$. Substituting in this equation the first order approximation (10) and neglecting terms of a higher order than $O(\varepsilon^2)$ yields:

$$r^{\mathrm{R}}(L)+ir^{\mathrm{I}}(L) = i\tilde{\kappa}_1 L + \int_0^L \Bigg[c_1(z) + c_2(z)\,e^{i\tilde{\kappa}_- z}\int_0^{z'} c_5(z')\,e^{-i\tilde{\kappa}_- z}\,\mathrm{d}z' + c_3(z)\,e^{-2i\tilde{\kappa}_1 z}\int_{z'}^L c_3(z')\,e^{2i\tilde{\kappa}_1 z}\,\mathrm{d}z' + c_4(z)\,e^{-\tilde{\kappa}_+ z}\int_{z'}^L c_7(z')\,e^{i\tilde{\kappa}_+ z}\,\mathrm{d}z' \Bigg]\mathrm{d}z. \tag{12}$$

This equation provides a solution for the transmissivity for fast P_1-waves. Using next the assumption that the thickness L of the stack of layers is much larger than the wavelength and all correlation distances involved, the limits

$$\Psi = \lim_{L\to\infty}\frac{r^{\mathrm{I}}(L)}{L}, \quad \gamma = -\lim_{L\to\infty}\frac{r^{\mathrm{R}}(L)}{L}, \tag{13}$$

are evaluated for stationary random media. Because of the self-averaging property, these limits are equal to their statistically averaged values. Thus, it is possible to use properties of ensemble averaging to express the attenuation coefficient and the phase increment in terms of just a few statistical parameters of the medium fluctuations. Due to the averaging, random functions are replaced by their expectation values. In the same way, the products of any two of these functions are substituted by the respective auto- and cross-correlation functions. Since the medium fluctuations are stationary functions of depth, their expectation values are independent of depth and their correlation functions depend only on the depth increment $\delta = z-z'$. The indicated calculations give both Ψ and γ as functions of the auto- and cross-correlations of the medium fluctuations:

$$\Psi = \kappa_1^{\mathrm{R}} + A - \int_0^\infty \Phi(\delta/a)\Bigg[\sqrt{2}B\exp(-\delta\kappa_-^{\mathrm{I}})\cos\left(\delta\kappa_-^{\mathrm{R}}-\frac{\pi}{4}\right) + \sqrt{2}B\exp(-\delta\kappa_+^{\mathrm{I}})\cos\left(\delta\kappa_+^{\mathrm{R}}-\frac{\pi}{4}\right) + C\exp(-2\delta\kappa_1^{\mathrm{I}})\sin(2\delta\kappa_1^{\mathrm{R}})\Bigg]\mathrm{d}\delta, \tag{14}$$

$$\gamma = \kappa_1^{\mathrm{I}} + \int_0^\infty \Phi(\delta/a)\Bigg[-\sqrt{2}B\exp(-\delta\kappa_-^{\mathrm{I}})\cos\left(\delta\kappa_-^{\mathrm{R}}+\frac{\pi}{4}\right) - \sqrt{2}B\exp(-\delta\kappa_+^{\mathrm{I}})\cos\left(\delta\kappa_+^{\mathrm{R}}+\frac{\pi}{4}\right) + C\exp(-2\delta\kappa_1^{\mathrm{I}})\cos(2\delta\kappa_1^{\mathrm{R}})\Bigg]\mathrm{d}\delta. \tag{15}$$

In results (14) and (15) we introduced three new quantities, A, B and C [see eqn (20)]. They

are linear combinations of the variances of the medium fluctuations. The superscripts R and I define the real and imaginary parts of the wavenumbers, e.g., $\tilde{\kappa}_1 = \kappa_1^R + i\kappa_1^I$. We assume only one correlation function $\Phi(\delta/a)$ with a single correlation length a for all fluctuations.

The calculation of eqns (14) and (15) can be performed for any integrable correlation function $\Phi(\delta/a)$. As long as the correlation function is rapidly decreasing for an increasing argument, any kind of function yields basically the same low-frequency behavior of the inter-layer flow ($\gamma_{\text{flow}} \propto \omega^{1.5}$) and the scattering attenuation ($\gamma_{\text{scatt}} \propto \omega^2$, 1-D-Rayleigh scattering). In the case of exponential media, the attenuation above ω_0 is found to be $\gamma_{\text{flow}} \propto \omega^{0.5}$ and $\gamma_{\text{scatt}} = \text{const}$. On the other hand, periodic media behave completely differently. Their correlation function is not a rapidly vanishing function of its argument, and inter-layer flow attenuation for low frequencies is proportional to $\gamma_{\text{flow}} \propto \omega^2$ (Gurevich *et al.*, 1997). There is no scattering attenuation and dispersion in periodic media, but pass and stop bands can be observed. For the calculation of (14) and (15) we choose an exponential correlation function, $\Phi(\delta/a) = \exp(-\delta/a)$. Exponential correlation functions of fluctuations of velocity and density, and thus of the poroelastic constants, are often observed in seismic practice (White *et al.*, 1990).

PHASE VELOCITY AND ATTENUATION

The result for the phase velocity reads for an exponential correlation function [integration of eqn (14)]:

$$\frac{\omega}{V_P} = \kappa_1^R + A - \frac{Ba(1+a(\kappa_-^R+\kappa_-^I))}{1+2a\kappa_-^I+a^2(\kappa_-^{R^2}+\kappa_-^{I^2})} - \frac{Ba(1+a(\kappa_+^R+\kappa_+^I))}{1+2a\kappa_+^I+a^2(\kappa_+^{R^2}+\kappa_+^{I^2})} - \frac{2Ca^2\kappa_1^R}{1+4a\kappa_1^I+4a^2(\kappa_1^{R^2}+\kappa_1^{I^2})}. \quad (16)$$

The corresponding attenuation coefficient [integration of eqn (15)] is given by:

$$\gamma = \kappa_1^I + \frac{Ba(1-a(\kappa_-^R-\kappa_-^I))}{1+2a\kappa_-^I+a^2(\kappa_-^{R^2}+\kappa_-^{I^2})} + \frac{Ba(1-a(\kappa_+^R-\kappa_+^I))}{1+2a\kappa_+^I+a^2(\kappa_+^{R^2}+\kappa_+^{I^2})} + \frac{Ca(1+2a\kappa_1^I)}{1+4a\kappa_1^I+4a^2(\kappa_1^{R^2}+\kappa_1^{I^2})}. \quad (17)$$

These results are valid under the assumption of small fluctuations, neglecting terms of $O(\varepsilon^3)$ and higher, but they are not restricted by any relationship between the wavelength and the correlation distance of the medium fluctuations and thus define "dynamic equivalent medium parameters". Equation (14)–(17) are independent of any kind of low frequency assumption even with respect to Biot's critical frequency (if a suitable Darcy coefficient $\tilde{q}$ is chosen, see Biot, 1962).

Whereas the wavenumbers of Biot's fast and slow wave are known for all frequencies (given below), the new constants A, B, and C are rather complicated functions of frequency and of the numerous auto- and cross-correlation functions. For a better understanding of the implications of these results, we introduce here an approximate solution, valid in the frequency range below Biot's critical frequency ω_c (usually, $\omega_c \gg \omega_0$). Assuming that $v = \omega/\omega_c \ll 1$, the small parameter v can be used for series expansions of the constants A, B, and C. Since attenuation and dispersion due to inter-layer flow and scattering are observable in most media for frequencies $\omega \ll \omega_c$, it is possible to neglect terms of $O(v^3)$ and higher (like permeability fluctuations) in the various series expansions. Since for $v \ll 1$ it always holds that

$$\kappa_2^R \gg \kappa_1^R \gg \kappa_1^R = \frac{\omega^2}{2\omega_c}\sqrt{\frac{\varrho}{H}\frac{\varphi\varrho}{\varrho_f}}\left(\frac{\varrho_f}{\varrho}-\frac{\alpha M}{H}\right)^2, \tag{18}$$

we assume that $\tilde{\kappa}_+ \approx \tilde{\kappa}_2$ and $\tilde{\kappa}_- \approx \tilde{\kappa}_2$. Further, $\tilde{\kappa}_2 \approx (1+i)\kappa_2$ and $\tilde{\kappa}_1 \approx \kappa_1^R = \kappa_1$. The wavenumbers κ_1, κ_2 are defined by $\kappa_1 = \omega\sqrt{\varrho/H}$ and $\kappa_2 = \sqrt{\omega\omega_c\varrho_f/2\varphi N}$. For convenience, A, B, and C keep their names after being expanded in a truncated series. These approximations were proposed first by Gurevich and Lopatnikov (1995). As a specific example, we study a medium that exhibits fluctuations of the frame modulus P_d, the Biot constant α, and the fluid bulk modulus (contained in M). Strong variations in the fluid bulk modulus can be observed in the presence of partial saturation: a small amount of gas in the fluid significantly reduces its effective bulk modulus which is defined by

$$K_f = \frac{K_{\text{liquid}}K_{\text{gas}}}{SK_{\text{gas}}+(1-S)K_{\text{liquid}}}. \tag{19}$$

For these fluctuations the constants A, B, and C are calculated as outlined above and read:

$$A = \frac{\omega}{2}\sqrt{\frac{\varrho}{H_0}}\frac{P_0}{H_0}\left(\sigma_{PP}^2+\frac{\alpha_0^2M_0}{P_0}(\sigma_{MM}^2+2\sigma_{P\alpha}^2)+\frac{\alpha_0^4M_0^2}{P_0^2}\sigma_{\alpha\alpha}^2\right),$$

$$\frac{2B}{\kappa_2} = \frac{\omega}{2}\sqrt{\frac{\varrho}{H_0}}\frac{P_0\alpha_0^2M_0}{H_0^2}$$
$$\cdot\left(\sigma_{PP}^2-2\sigma_{PM}^2+\sigma_{MM}^2-2\frac{P_0-\alpha_0^2M_0}{P_0}(\sigma_{P\alpha}^2-\sigma_{M\alpha}^2)+\frac{(P_0-\alpha_0^2M_0)^2}{P_0^2}\sigma_{\alpha\alpha}^2\right),$$

$$\frac{C}{2\kappa_1} = \frac{\omega}{8}\sqrt{\frac{\varrho}{H_0}}\frac{P_0^2}{H_0^2}$$
$$\cdot\left(\sigma_{PP}^2+2\frac{\alpha_0^2M_0}{P_0}(\sigma_{PM}^2+2\sigma_{P\alpha}^2)+\frac{\alpha_0^4M_0^2}{P_0^2}(\sigma_{MM}^2+4\sigma_{\alpha\alpha}^2+4\sigma_{M\alpha}^2)\right). \tag{20}$$

With these constants, keeping in mind the frequency dependence of $\kappa_1 \propto \omega$, $\kappa_2 \propto \sqrt{\omega}$, it is easy to see that the phase velocity has three limiting values that may be called a quasi-static velocity $V_{qs} = \omega[\kappa_1+A]^{-1}$ for $\omega \to 0$, an intermediate no-flow velocity $V_{nf} = \omega[\kappa_1+A-2B/\kappa_2]^{-1}$ for $\omega \gg \omega_0$ but wavelengths smaller than the correlation length a, and finally a ray-theoretical limit $V_{\text{ray}} = \omega[\kappa_1+A-2B/\kappa_2-C/(2\kappa_1)]^{-1}$ above that limit (but necessarily below Biot's ω_c). A more detailed discussion of these limiting velocities, including their different anisotropic behavior for non vertical incidence, can be found in Gelinsky and Shapiro (1997b).

For a heterogeneous sediment model consisting of a stack of layers with average properties close to that of water-saturated Berea sandstone (Norris, 1993), we calculated phase velocity and attenuation $Q^{-1} = 2\gamma/\kappa_1$ both as a function of frequency, normalized by Biot's critical frequency. Here, the theoretical results are examined (Figs 1 and 2) and in the next section they are compared with the numerical results (Figs 3 and 4). The model discussed in Figs 1–4 has 30% fluctuations in μ_d, 25% in K_d, 15% in K_f, as well as 5% in ϱ and 1% in K_g. This corresponds to P-velocity fluctuations of almost 14%. The variation of K_f with depth is caused by partial gas saturation (2% gas). Here it is assumed that the fluctuations of K_f and K_d are uncorrelated. The effects of correlation between K_f and K_d are addressed below in the section on partial saturation. The medium can be described with the following variances: $\sigma_{PP}^2 = 0.0719$, $\sigma_{MM}^2 = 0.0267$, $\sigma_{\alpha\alpha}^2 = 0.0128$, $\sigma_{PM}^2 = 0.0319$, $\sigma_{M\alpha}^2 = -0.0135$, $\sigma_{P\alpha}^2 = -0.0304$. The corresponding average values are: $P_0 = 2.89\cdot10^{10}$ Pa, $M_0 = 1.12\cdot10^{10}$ Pa, and $\alpha_0 = 0.67$. The resulting phase velocity [eqn (16)] and its three

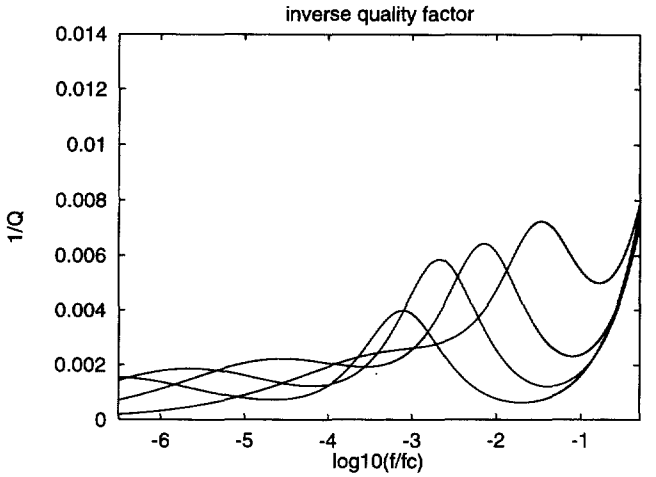

Fig. 1. Inverse quality factor as function of frequency, normalized by Biot's critical frequency $f_c = 1.1 \times 10^5$ Hz for the model described in the text. From the left to the right peak, the correlation length a is 3.5, 1.25, 0.37, 0.08 m. Attenuation due to inter-layer flow dominates for the lowest frequencies. The significant peaks in an intermediate frequency range are caused by poroelastic scattering. Biot's global flow attenuation begins to be important for the highest frequencies.

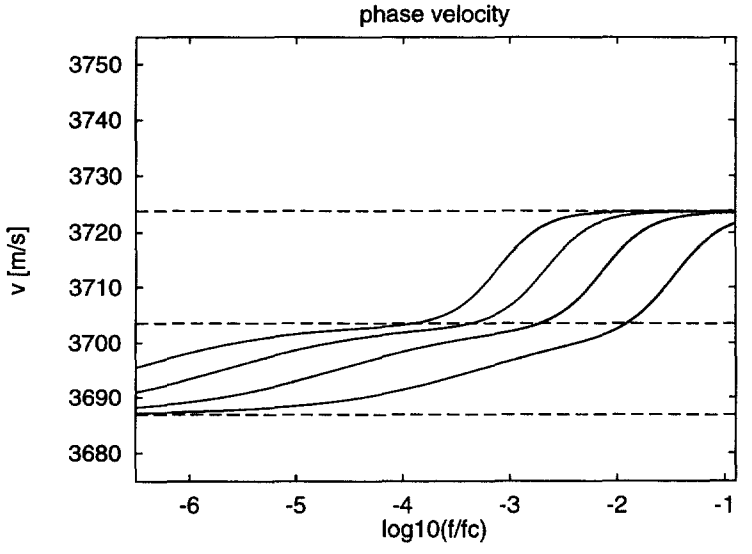

Fig. 2. Phase velocities for the same model as in Fig. 1. The curves correspond (from left to right) to correlation lengths a of 3.5, 1.25, 0.37, 0.08 m. The limiting velocities as defined in the text are plotted with dashed lines. For lowest frequencies, the velocities asymptotically approach the limiting value V_{gs}, the intermediate frequency range is characterized by V_{nf}, and the high frequency limit is given by V_{ray}.

limiting values are plotted in Fig. 2 and the attenuation Q^{-1} [based on eqn (17)] is shown in Fig. 2. Biot's critical frequency for this model is $\omega_c = 2\pi \times 1.1 \times 10^5\ \text{s}^{-1}$. Thus, the surface seismic frequency range can be found approximately between -4 and -3 on the logarithmic frequency scales. The correlation lengths (exponential correlation function) considered in Figs 1 and 2 range from 3.5 m down to 8 cm (curves from left to right: $a = 3.5$, 1.25, 0.37, and 0.08 m). For the thicker layers ($a = 3.5$, 1.25 m), the inter-layer flow cannot equilibrate the pressure at seismic frequencies—the maximum of inter-layer flow attenuation is below 1 Hz. For the thinner layers ($a = 0.37$, 0.08 m), a rather continuous change from the quasi-static to the ray theoretical velocity limit can be observed. This high frequency limit is

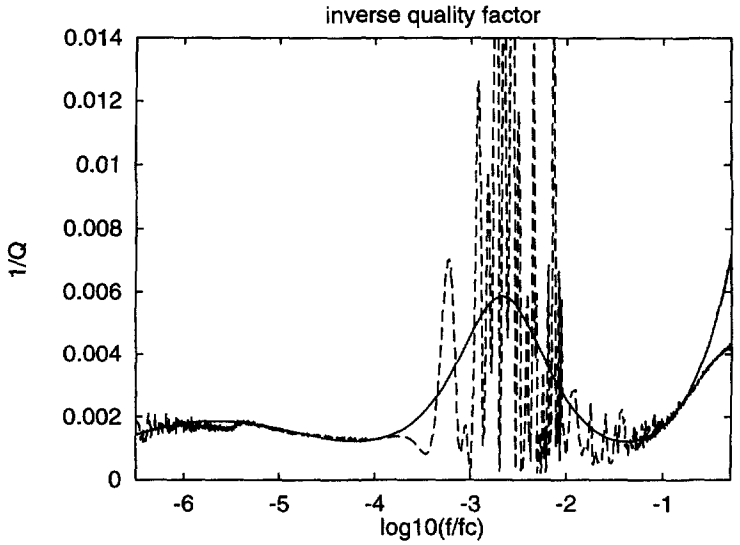

Fig. 3. Comparison of theory (solid line) and numerical result (dashed line) for the inverse quality factor. The model parameters are the same as in Fig. 1 and given in the text. The correlation length a is 1.25 m.

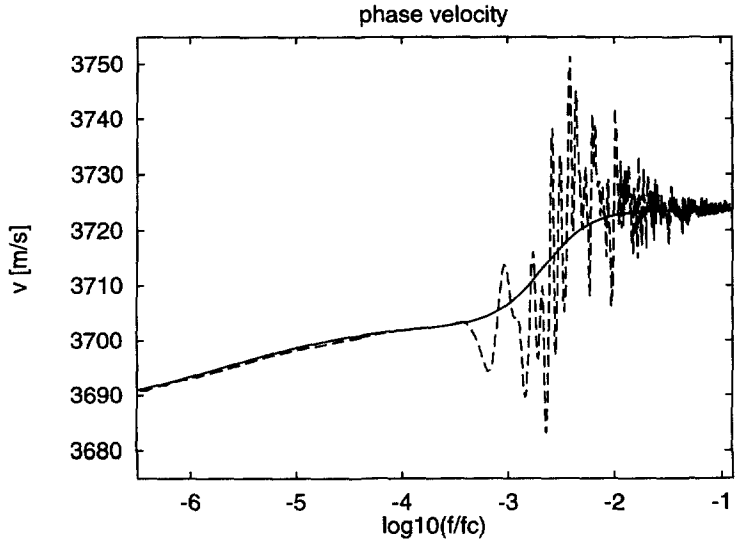

Fig. 4. Comparison of numerical result (dashed line) with theory (solid line) for the phase velocity. The model parameters are the same as in Fig. 2 and given in the text. The correlation length a is again 1.25 m.

slightly affected by global flow dispersion. For the larger correlation lengths, the peaks of scattering and inter-layer flow attenuation can be distinguished. Attenuation due to the Biot global flow becomes relevant above $\omega/\omega_c \approx 10^{-2}$.

NUMERICAL RESULTS

The analytical results were verified by numerical modeling with the OASES software (Schmidt and Tango, 1986) which numerically simulates the linear dynamics of horizontally layered poroelastic systems using an advanced version of the propagator matrix—reflectivity approach. In the present study, OASES software was used to compute transmission coefficients of elastic waves propagating in a typical, finely-layered poroelastic structure.

These transmission coefficients were then used to reconstruct attenuation coefficients and phase velocities as function of frequency. The investigation of poroelastic structures is possible using the so-called Biot extension of OASES that allows layers to be poroelastic, fluid or gas saturated, and interacting (open-pore boundary conditions at interfaces).

The model that was used to compare theory and numerical results consisted of 100 layers. A larger number of layers would make the numerical results smoother and, in the limit of an infinite number of layers, the numerical result should exactly equal the theoretical prediction. However, the absolute transmissivity of the stack of layers decreases with an increasing stack thickness, prohibiting a reasonable determination of phase and attenuation for more than approximately 500 layers. Due to the finite thickness of the numerical model, both attenuation and phase velocity results show many random oscillations due to constructive and destructive interference. These oscillations (which can also be observed in purely elastic models, Shapiro and Hubral, 1996) can be found mainly between 100 Hz and 10 kHz where (poro-)elastic scattering is strongest and the seismic wavelength is comparable to the correlation length.

Figure 3 shows the inverse quality factor for this model. The solid line marks the theoretical result and the dashed line is derived from the numerical results. The correlation length is 1.25 m, all other parameters are the same as those defined above. The theory and numerical experiments are in excellent agreement over the whole frequency range up to approximately 10% of Biot's critical frequency. For higher frequencies the underlying low frequency approximations are not justified. Especially the assumption that the Biot global flow attenuation is proportional to $(\omega/\omega_c)^2$ is not adequate in this frequency range, cf Fig. 3. Figure 4 features the corresponding plot of the phase velocity, again for a correlation length of 1.25 m. The numerical phase velocity curve (dashed line) shows the same random oscillations between approximately 100 Hz and 10 kHz as does the attenuation (Fig. 3). Otherwise, the agreement between the theory and the numerical experiments is excellent over the whole frequency range. Our numerical experiments further demonstrated that the results are rather insensitive to density fluctuations and that their omission in the analytical formulas (20) (leading to a significant simplification) is fully justified.

The theory in its present form is limited to the description of plane waves that are vertically incident on a horizontal stack of layers. A generalization to non-vertical incidence and dipping layers is possible but would strongly complicate the analytical calculations. We simulated non vertical incidence numerically and found that our theory is well applicable in its present form even for angles of incidence that differ by more than 20° from vertical incidence.

PARTIAL SATURATION

In two different models (Figs 5 and 6) the effect of partial saturation on attenuation is studied in more detail. This also helps to understand the mechanism of inter-layer flow more clearly. Before (Figs 1–4) the fluctuations of saturation [i.e., of the fluid bulk modulus (19)] and of the poroelastic constants were uncorrelated, making $\sigma^2_{K_d K_f} = 0.004$ very small. Figure 5 now shows the results for gas bubbles being located mainly in the more compressible part of the presence ($\sigma^2_{K_d K_f} = 0.04$), and Fig. 6 depicts the opposite case—gas accumulated mainly in the stiffer layers ($\sigma^2_{K_d K_f} = -0.04$). The corresponding σ^2_{MM}, σ^2_{PM}, and $\sigma^2_{M\alpha}$ are given in the figure captions. A compressional wave that propagates through the stack of layers tends to squeeze fluid out of the weaker (more compliant) layers into the stiffer layers with a less deformable porespace. The efficiency of this mechanism is reduced if gas occupies the weaker porespace (Fig. 5) and enhanced in the opposite case (Fig. 6). Also the impedance contrast is affected by the distribution of gas: if gas is located predominantly in the softer layers and water in the stiffer layers, the impedance contrast is increased as compared to homogeneous saturation. Accordingly, the attenuation due to scattering (Fig. 5) is increased. The opposite effect can be observed in Fig. 6. Scattering, however, is much less affected by partial saturation than the inter-layer flow.

Also, the velocity dispersion is a function of partial saturation and is influenced by the way its fluctuations are correlated with those of the poroelastic constants. For lowest

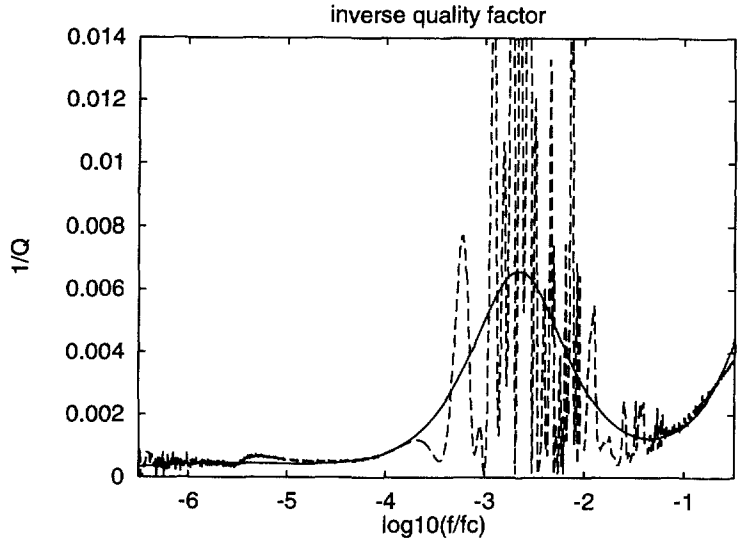

Fig. 5. Reduced inter-layer flow attenuation for a model with gas mainly in the softer portion of the porespace. With the exception of the correlation of gas saturation and poroelastic fluctuations, the model is the same as that in Fig. 3. Here, $\sigma_{MM} = 0.0542$, $\sigma_{PM} = 0.0625$, $\sigma_{M\alpha} = -0.0264$. The numerical result is given with a dashed line, the theoretical prediction with a solid line.

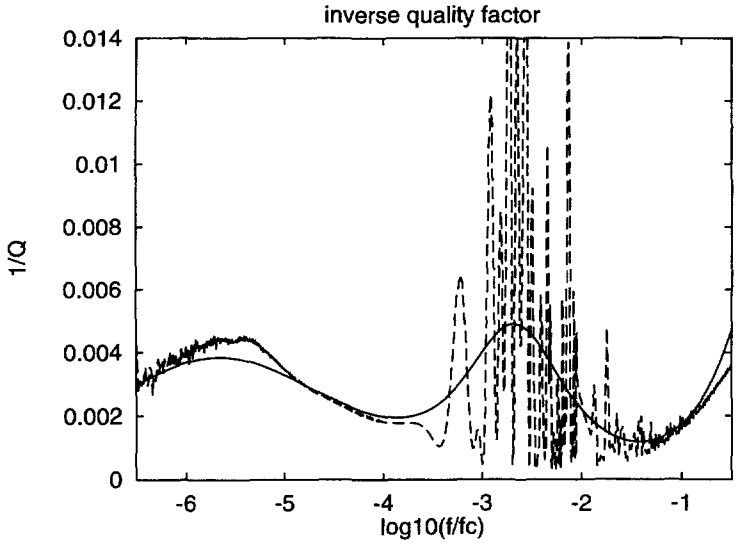

Fig. 6. Enhanced inter-layer flow attenuation for gas mainly in the less compressible porespace. The numerical result is given with a dashed line, the theoretical prediction with a solid line. The parameters are the same as in the previous model, with the exception of: $\sigma_{MM} = 0.0005$, $\sigma_{PM} = -0.0063$, $\sigma_{M\alpha} = 0.0026$. All plots are explained in more detail in the text.

frequencies the inter-layer flow (if present like in the model of Fig. 6) squeezes water into the less compressible porespace, making V_{qs} the same regardless where the gas had accumulated. For frequencies around ω_0 and higher, however, the impedance difference and the absence (or presence) of inter-layer flow significantly affects the velocity. The influence of this effect on the limiting velocities V_{qs}, V_{nf}, and V_{ray} and their anisotropy is illustrated and discussed in more detail in Gelinsky and Shapiro (1997b).

CONCLUSIONS

An extension of the generalized O'Doherty–Anstey formalism for poroelasticity has been derived. This new theory then has been applied to describe attenuation and dispersion

of seismic waves in saturated, layered sediments. The theoretical predictions of significant attenuation and some dispersion due to the heterogeneity could be verified by comparison with numerical results derived with a propagator matrix—reflectivity approach.

In layered, saturated sediments dispersion and attenuation depend on frequency and on fluctuations of the poroelastic parameters, permeability, and on fluid properties like the bulk modulus, density, and viscosity. The resulting dynamic-equivalent medium model gives the *P*-wave phase velocity and the attenuation coefficient in the full frequency range from the quasi-static to the ray theoretical limit, including the no-flow-regime for intermediate frequencies. Its results are in excellent agreement with independent numerical studies. Since the new theory utilizes a fully analytical model, it provides a fast means for upscaling of acoustic velocities to lower frequencies, utilizing, e.g., velocities measured from core samples to predict sonic log velocities or those in the surface seismic frequency range.

Unlike earlier studies, here the combined effects of scattering and fluid flow are treated together from first principles. The attenuation in comparison to homogeneous systems is strongly enhanced. In addition to Biot's global flow, *P*-waves are attenuated in heterogeneous media due to scattering and inter-layer flow. These results suggest that a great part of the attenuation that can be observed in porous saturated sedimentary rocks at seismic frequencies is caused by scattering and local flow on macroscopic length scales defined by the layering. The various attenuation mechanisms are found to be approximately additive. The inter-layer flow effect contributes significantly to the total attenuation in the seismic frequency range, especially for thin layers (with correlation length of centimeters) with high permeability. Elastic scattering is mainly caused by heterogeneities on larger scales (correlation length of several meters). It is important over a broad frequency range from seismic to sonic frequencies. Biot's global flow (the relative displacement of solid frame and fluid) contributes mainly for ultrasonic frequencies.

Acknowledgements—Early on, this project was encouraged by R. White of Birkbeck College, London. It was continued in Karlsruhe during the German–Norwegian Project, Phase II, financed by STATOIL (Norway) and the German BMBF. S. Gelinsky is grateful to Western Atlas Logging Services for giving him the opportunity to finish and publish this work. He thanks also Karen Bush for proof-reading and valuable suggestions. S. Shapiro and T. Müller thank the German Research Foundation for funding. The authors thank M. Stern from the University of Texas at Austin for providing them with the poroelastic extension of OASES.

REFERENCES

Aki, K. and Richards, P. G. (1980) *Quantitative Seismology*, pp. 163–167, 267–270. W. H. Freeman and Co., New York.

Biot, M. (1962) Mechanics of deformation and acoustic propagation in porous media. *Journal of Applied Physics* **33,** 1482–1498.

Chandler, R. and Johnson, D. L. (1981) The equivalence of quasi-static flow in fluid saturated porous media and Biot's slow wave in the limit of zero frequency. *Journal of Applied Physics* **52,** 3391–3395.

Gelinsky, S. and Shapiro, S. A. (1997a) Dynamic-equivalent medium model for thinly layered saturated sediments. *Geophys. J. Int.* **128,** F1–F4.

Gelinsky, S. and Shapiro, S. A. (1997b) Poroelastic Backus-averaging for anisotropic layered fluid and gas saturated sediments. *Geophysics* **62,** 1867–1878.

Gurevich, B., Zyrianov, V. B. and Lopatnikov, S. L. (1997) Seismic attenuation in finely layered porous rock. *Geophysics* **62,** 319–324.

Gurevich, B. and Lopatnikov, S. L. (1995) Velocity and attenuation of elastic waves in finely layered porous rocks. *Geophys. J. Int.* **121,** 933–947.

Gurevich, B. and Schoenberg, M. (1997) Boundary conditions at open or partially closed interfaces in porous media. 59th Conference Eur. Assn. Expl. Geophys., Extended Abstracts, paper F012.

Gurevich, B. and Schoenberg, M. (1998) Interface conditions for Biot's equations of poroelasticity. *Journal of the Acoustical Society of America*, submitted.

Norris, A. N. (1993) Low-frequency dispersion and attenuation is partially saturated rocks. *Journal of the Acoustical Society of America* **94,** 359–370.

Plona, T. J. (1980) Observation of a second bulk compressional wave in a porous medium at ultrasonic frequencies. *Applied Physics Letters* **36,** 259–261.

Rasolofosaon, P. N. J. (1988) Importance of interface hydraulic condition on the generation of second bulk compressional wave in porous media. *Applied Physics Letters* **52,** 780–782.

Schmidt, H. and Tango, G. (1986) Efficient global matrix approach to the computation of synthetic seismograms. *Geophysical Journal of the Royal Astronomical Society* **84,** 331–359.

Shapiro, S. A. and Hubral, P. (1996) Elastic waves in thinly layered sediments: the equivalent medium and generalized O'Doherty–Anstey formulas. *Geophysics* **61,** 1282–1300.

Shapiro, S. A. and Müller, T. (1998) Seismic signatures of permeability in heterogeneous porous media. *Geophysics*, submitted.

Sheng, P. (1995) *Introduction to Wave Scattering, Localization, and Mesoscopic Phenomena*. Academic Press, New York.

White, B., Sheng, P. and Nair, B. (1990) Localization and backscattering spectrum of seismic waves in stratified lithology. *Geophysics* **55**, 1158–1165.

White, J. (1983) *Underground Sound, Application of Seismic Waves*. Elsevier.